

SEMICONDUCTOR-SEMIMETAL TRANSITIONS IN InAs-GaSb SUPERLATTICES*

L. L. Chang

IBM T. J. Watson Research Center
 Yorktown Heights, New York USA

Semiconductor-semimetal transitions with variations in layer thicknesses and magnetic fields have been investigated in InAs-GaSb superlattices. Experimental results cover the entire semimetallic regime from the semiconductor limit to the heterojunction limit.

I. Introduction

A semiconductor superlattice refers to a periodic structure along one dimension, which is made of alternating layers of two semiconductors [1]. The period in thickness typically lies in the range from tens to hundreds of angstroms. The superlattice potential modifies significantly the band structure of the host semiconductors, creating minizones in wavevector and subbands in energy. The main objective for making the man-made superlattice is to pursue this basic quantization phenomenon and to investigate its ensuing electronic properties.

Two systems of superlattices have been studied experimentally: GaAs-GaAlAs with which we started [2], and InAs-GaSb on which our current attention is focused [3]. The energy diagrams of the two systems are illustrated schematically in Fig.(1), where the superlattice potential in bandedges of the host semiconductors are plotted along the direction perpendicular to the plane of the layers. The quantum states or subbands are designated as E_{le} and E_{lh} for electrons and heavy holes, respectively; their difference is defined as the energy gap, E_{gs} , of the superlattice. Only the ground subbands are shown here; those occurring at higher energies and those belonging to light holes,

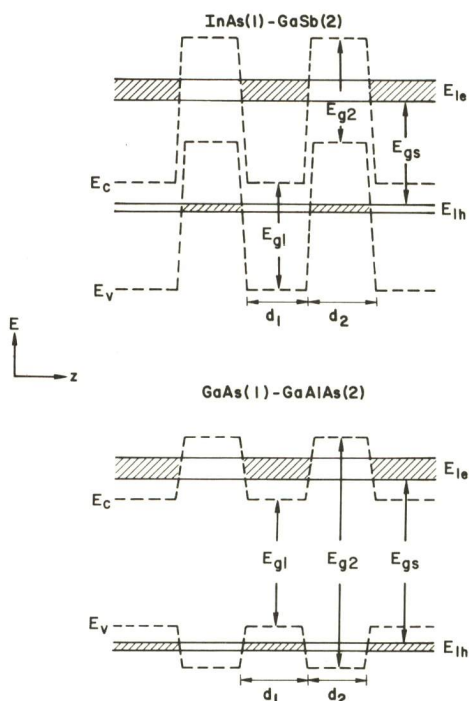


Fig.(1) Schematic energy diagrams of the superlattice systems

which are of secondary importance in this work, having been neglected for simplicity. As the superlattice potential is varied, both the energies and widths of the subbands and the dimensionality of their associated electrons are changed. Various observations, using different experimental techniques with focus on different aspects, such as energy dispersion, density of states and Fermi surface, have been reported, as summarized in recent reviews [4,5].

While the two systems have many similarities, important differences exist. Unlike GaAs-GaAlAs where both electrons and holes are confined in GaAs as indicated by shaded regions in Fig.(1), electrons are concentrated in InAs and holes in GaSb in the present system. Another difference, perhaps more significant, is the existence of an energy range between E_{c1} and E_{v2} in the InAs-GaSb system where both electrons and holes can be present simultaneously. As the layer thickness increases, E_{gs} decreases and may become zero and eventually negative, in contrast to the situation in GaAs-GaAlAs where E_{gs} is limited to E_{c1} . The superlattice then behaves as a semimetal^{gs} with electron transfers to the conduction band of InAs from the valence band of GaSb where an equal number of holes are generated. In this work, we are primarily concerned with superlattices in the semimetallic regime, presenting their transport properties under magnetic fields for a wide range of layer thickness.

II. Theoretical Consideration

The subband structure of the superlattice can be obtained by wavefunction matching along the z-direction. However, unlike the situation in GaAs-GaAlAs where plane waves can be used because of the wide separation of E_c and E_v , the close vicinity of E_{c1} and E_{v2} in InAs-GaSb calls for the utilization of Bloch functions in the v_2^k -p framework, coupling electrons and light holes [3]. Similar results have also been obtained from LCAO calculations [6]. In addition, semi-three-dimensional computations in the range of thin layers have been reported with both the tight-binding and the pseudopotential techniques [7,8].

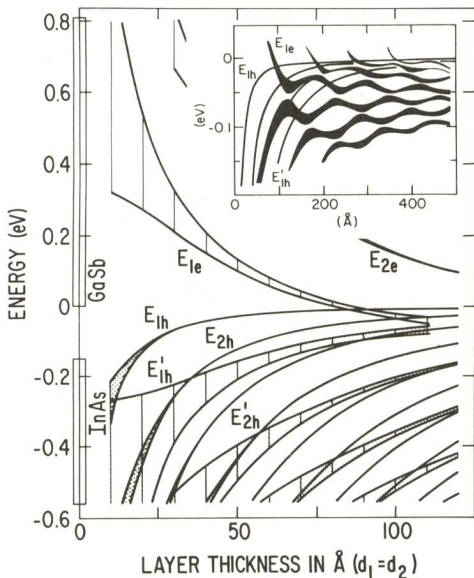


Fig.(2) Calculated subband energies of electrons, and heavy and light holes

Figure (2) shows the LCAO results, using $d_1=d_2$ and $E_{v2}-E_{c1}=150$ meV as obtained from absorption measurements [5]. It is clear that as the layer is widened, E_{gs} decreases and both E_{lh} and E_{lh}' , the subbands of light holes, increase. The crossover of E_{1e} and E_{1h}' occurs at a critical thickness of 185\AA , corresponding to the semiconductor-semimetal transition. The inset diagram illustrates the situations in the range of thick layers to indicate that the negative E_{gs} does not increase monotonically because of interactions of electrons and light holes. In the semimetallic regime, however, the effect of electron transfer on the subband structure has to be taken into account.

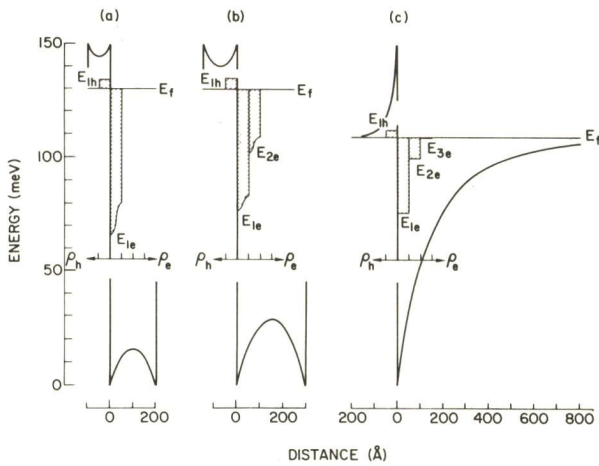


Fig.(3) Calculated potentials of superlattices (a) and (b), and the heterojunction (c): Subband energies and densities of states are shown in the middle (hatched)

The flow of electrons from GaSb to InAs causes band bending, which in turn affects the subband energies by pushing E_e upward and E_h downward. A self-consistent solution can be obtained by using the Thomas-Fermi approximation to calculate the band bending [9], the LCAO method to compute the subbands, and the quasi two-dimensional density of states to determine the Fermi energy with the constraint of charge neutrality. Results obtained in this fashion are shown in Fig. (3a,b) for the superlattices, where the potentials are plotted at the top and bottom while the density of states in the middle, each unit representing $0.96 \times 10^{10} / \text{meV} \cdot \text{cm}^2$ for electrons and $1.4 \times 10^{11} / \text{meV} \cdot \text{cm}^2$ for heavy

holes. This procedure becomes rather tedious and inaccurate with increasing layer thickness when multiple subbands are involved, some of which begin to be localized near the interface. In the limit of very thick layers, the interaction between adjacent interfaces becomes negligible and the superlattice behaves in essence as a series of isolated heterojunctions. The subbands in this case can be similarly obtained by solving self-consistently the Schroedinger equation, as shown in Fig. (3c).

III. Semiconductor-to-Semimetal Transition with Thickness Variations

A large number of undoped superlattices were prepared on (100) GaSb substrates by molecular beam epitaxy. The initial evidence of the semiconductor-semimetal transition was provided from Hall measurements as shown in Fig. (4). The abscissa is the layer thickness of InAs, while that of GaSb, chosen somewhat arbitrarily in the samples, is usually equal or smaller. The exact value is of secondary importance, since it does not affect the subband structure significantly as a result of the heavy hole mass. It is evident that the concentration in Fig. (4) takes a sudden rise near 100Å , indicating the onset of carrier transfer in the semimetallic state in agreement with that predicted theoretically. The subsequent drop arises from the fact that the carriers become increasingly concentrated near the interface while those measured experimentally represent some average values over the entire layer. The mobilities in all the samples are rather high, greater than $10^4 \text{ cm}^2/\text{V} \cdot \text{sec}$, since the electrons, generated from the transfer process, do not suffer severely from impurity scattering.

Quantitative values of electron densities or Fermi energies have been obtained from transverse magneto-resistance measurements, as shown in Fig. (5) for the $200\text{-}100 \text{Å}$ sample. The resistance is quite high, as expected for a semimetal; an increase by a factor about 50 at high fields being typical in contrast to a few percent observed usually in semiconductors. A well-defined series of oscillations are

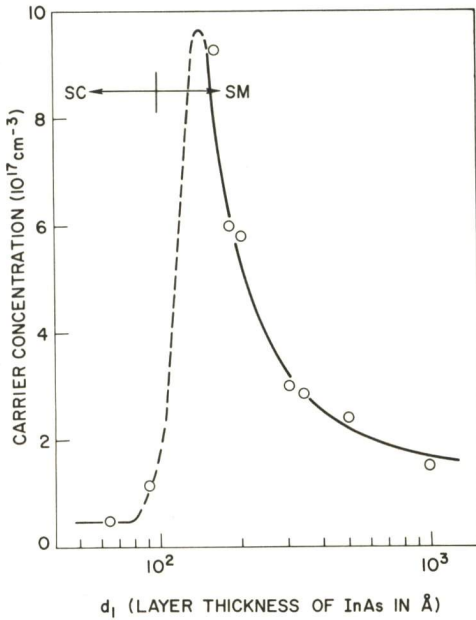


Fig.(4) Carrier concentration from Hall measurements at 4.2K vs the layer thickness of InAs to show the semiconductor-semimetal transition

clearly observed, particularly with the aid of derivative techniques. It starts at fields as low as 1T, because of the high electron mobilities. Measurements with fields parallel to the plane of the layers result in a featureless characteristic, as can be seen in Fig. (5). This demonstrates the quasi two-dimensional nature of the subband in the superlattice [11, 12].

The spectra of oscillations for samples with thick layers are shown in Fig. (6). The characteristics are generally more complex, showing additional features, particularly at high fields. These could be attributed to a number of possibilities, although their exact origins are not understood: Multiple subbands are involved which may contribute to additional oscillations; the finite dispersion or bandwidth of the subbands may result in complicated Fermi surfaces; the effect of electron spin, although it is expected to be small for energies high above the conduction bandedge of InAs [13], may not be completely negligible; and,

finally, the electron transfer process and thus the entire subband structure depend on the magnetic field as the Landau levels of both electrons and holes are successively crossed at the Fermi level, and such dependences become increasingly important at high fields. Nevertheless, if we neglect the details and concentrate on the main features in the low-field region below 5T, the oscillations appear to belong to a single series, similar to the situation in Fig. (5). Indeed, standard plots of the inverse fields of extrema vs integers invariably yield straight lines, from which the electron densities or Fermi energies can be evaluated. These electrons are

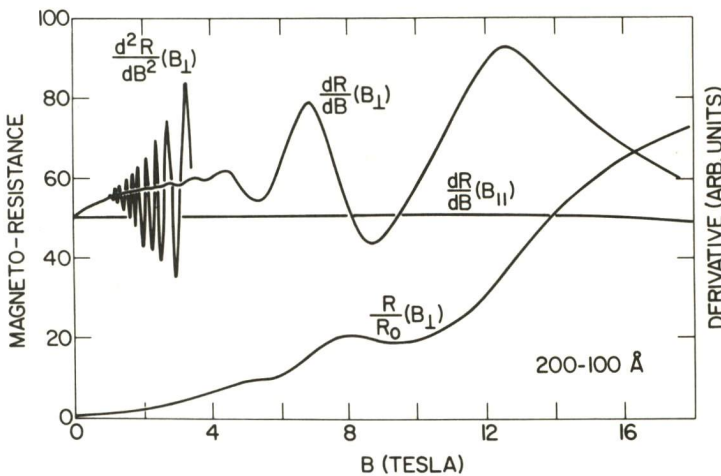


Fig.(5) Magneto-resistance and its derivatives at 4.2K to show Shubnikov-de Haas oscillations: Indicated are the orientations of the field and the InAs-GaSb layer thickness

these electrons are

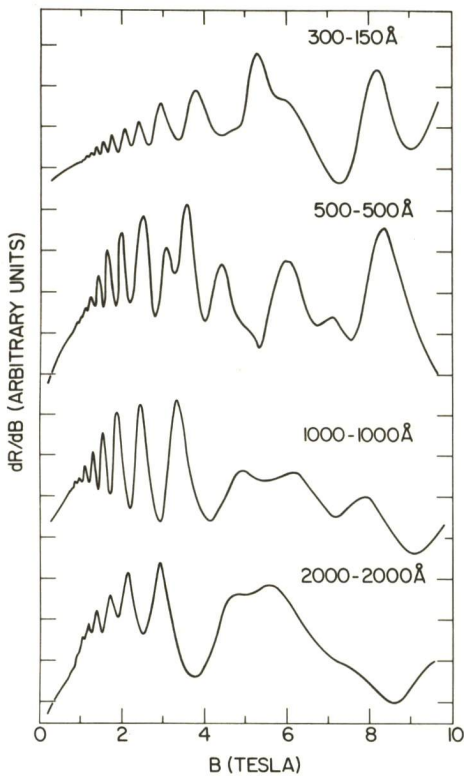


Fig.(6) Oscillations from superlattice samples with various InAs-GaSb layer thicknesses as indicated

expected to be associated with the ground states E_{1g} , because of their large Fermi energies.

The results are shown in Fig. (7) where the Fermi energy, defined with respect to E_{1g} , is plotted as a function of the layer thickness of InAs. In obtaining E_f , we have used an average effective electron mass of $0.028m_0$, a value enhanced by the nonparabolicity effect for the energy range under consideration. The choice of plotting E_f instead of the electron density is based on the reason that only the electron density associated with E_{1g} , not the total density, is measured experimentally. The thickness range covers the entire semimetallic regime, from the semiconductor limit to the heterojunction limit. The agreement with the few theoretical points obtained from Fig. (3), as described above, is surprisingly good, considering the crude nature of the calculations

which are meant to serve only as quantitative guidelines.

IV. Semimetal-to-Semiconductor Transition under Magnetic Fields

The semimetallic state originates from the relative subband positions of electrons and holes, $E_{1h} > E_{1g}$. The situation can be reversed under magnetic fields. The series of Landau levels of both electrons and holes are swept successively across E_f with increasing fields, resulting in a reverse transfer of electrons from InAs back to GaSb. In the quantum limit only the ground Landau levels are populated, as shown in Fig. (8) for an ideal semimetal. A further increase in fields causes their crossing as well to reach the condition of a semimetal-semiconductor transition. Subsequently, the superlattice behaves as a semiconductor, as semimetallic carriers

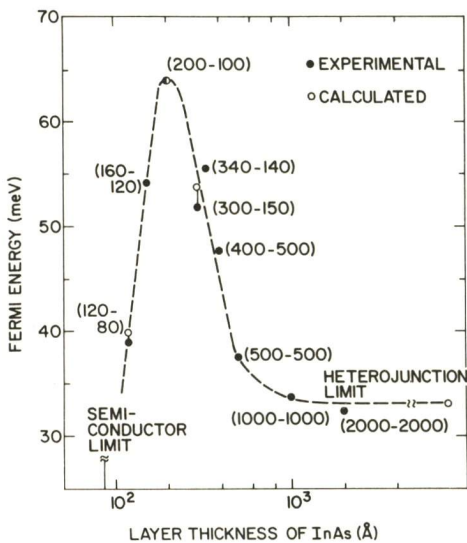


Fig.(7) Variations of the Fermi energy of superlattices throughout the semimetallic regime: Values given in parentheses are the layer thicknesses in angstroms of InAs-GaSb

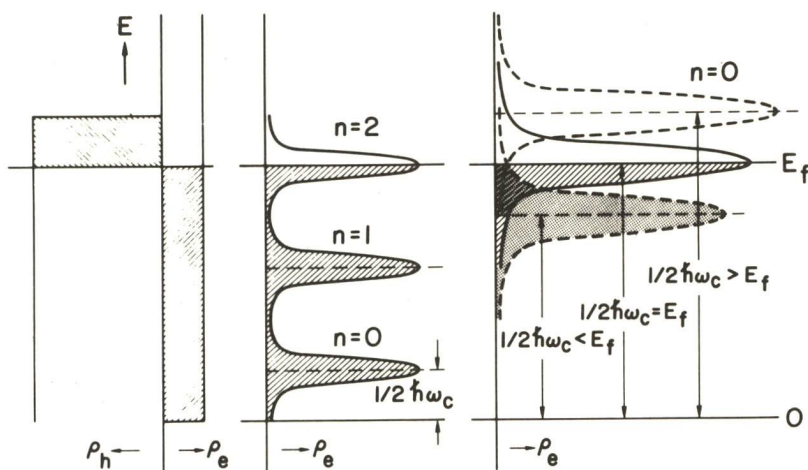


Fig.(8) Densities of states in an ideal two-dimensional semimetal: left, for electrons and heavy holes without magnetic fields; middle, for electrons at moderate fields; right, for electrons at the semi-metal-semiconductor transition

are depleted, accompanied by a reduction in conductivity [14].

This magnetic field-induced transition is expected to be quite a general property of semimetals [15]. The criterion for its observation requires that the cyclotron energy, $\hbar\omega_c/2$, be equal to E_f at moderate fields, which can be readily achieved with the superlattice whose subband structure can be controlled. The magneto-

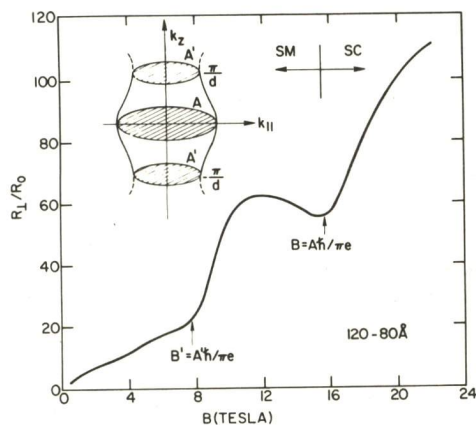


Fig.(9) Magneto-resistance vs field of the InAs-GaSb superlattice of the specified layer thickness: Arrows indicate calculated fields corresponding to the extremal areas of the Fermi surface shown in the inset. The semi-metal-semiconductor transition is indicated

resistance of the 120-80Å sample is shown in Fig. (9), together with its Fermi surface in the inset. The thin layer of InAs in this case gives rise to a significant dispersion in E_{1e} , resulting in an extremal cross section at the superlattice zone boundary $k_z = \pm\pi/d$ in addition to the usual one at the center. The experimental data reflect these features, showing two abrupt rises at fields in agreement with those calculated as indicated by arrows. The semi-metal-semiconductor transition is indicated at $B = A\hbar/\pi e$, after which the resistance tends to saturate without additional features. It is worth mentioning that, unlike the transition described in the previous section where semiconducting or semimetallic behaviors are obtained in different samples with different thicknesses, the present one is achieved within the same sample by the use of a magnetic field as the controlling parameter.

V. Recent Developments

While the semimetallic superlattice has been established from the observations of high magneto-resistance and enhanced carrier density, its direct demonstration was provided recently from magneto-absorption experiments in the far infrared region [16]. Figure (10) shows the energies at transmission minima vs fields for the 120-80Å sample in the usual fashion. The extrapolated energy to zero field

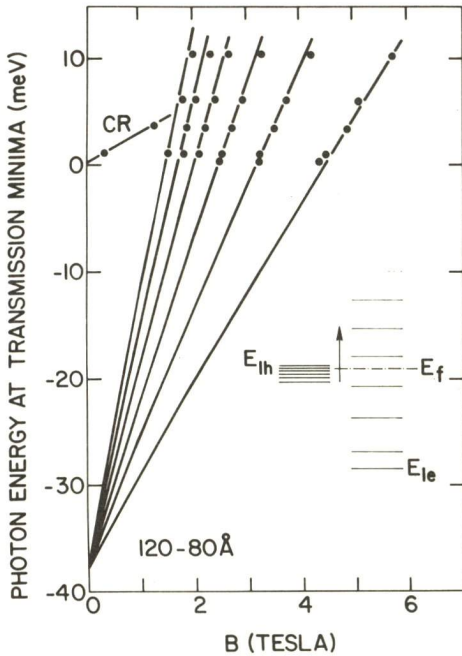


Fig.(10) Magneto-absorptions including cyclotron resonance (CR) and intersubband transitions as indicated in the inset

experiments are preliminary, they do point to the rapidly expanding and ever-stimulating nature of the superlattice.

Acknowledgment

The work presented here is the result of a group effort. I acknowledge valuable contributions from many of my colleagues and collaborators with whom I have had the privilege to co-author in the references.

References

- * Part of this work was performed at the Francis Bitter National Magnet Laboratory, which is supported at Massachusetts Institute of Technology by the National Science Foundation.
- 1) L. Esaki and R. Tsu: IBM J. Res. Develop. 14 (1970) 61.
 - 2) L. L. Chang, L. Esaki, W. E. Howard, R. Ludeke and G. Schul: J. Vac. Sci. Technol. 10 (1973) 655.
 - 3) G. A. Sai-Halasz, R. Tsu and L. Esaki: Appl. Phys. Lett. 30 (1977) 651.

- 4) L. L. Chang and L. Esaki: Prog. Crystal Growth Charact. 2 (1979) 3.
- 5) L. L. Chang and L. Esaki: Presented at 3rd Int. Conf. Electronic Properties of Two-Dimensional Systems, Lake Yamanaka, Japan, Sept. 1979 (to appear in Surf. Sci., 1980).
- 6) G. A. Sai-Halasz, L. Esaki and W. A. Harrison: Phys. Rev. B13 (1978) 2812.
- 7) A. Medhukar, N. V. Dandekar and R. N. Nucho: J. Vac. Sci. Technol. 16 (1979) 1507.
- 8) J. Ihm, P. K. Lam and M. L. Cohen: J. Vac. Sci. Technol. 16 (1979) 1512.
- 9) R. W. Keyes: Comments Solid State Phys. 7 (1976) 53.
- 10) L. L. Chang, N. J. Kawai, G. A. Sai-Halasz, R. Ludeke and L. Esaki: Appl. Phys. Lett. 35 (1979) 939.
- 11) L. L. Chang, H. Sakaki, C.-A. Chang, and L. Esaki: Phys. Rev. Lett. 38 (1977) 1489.
- 12) F. F. Fang and P. J. Stiles: Phys. Rev. 174 (1968) 823.
- 13) C. R. Pidgeon, D. L. Mitchell and R. N. Brown: Phys. Rev. 154 (1967) 737.
- 14) N. J. Kawai, L. L. Chang, G. A. Sai-Halasz, C.-A. Chang, and L. Esaki: Appl. Phys. Lett. 36 (1980) 369.
- 15) N. B. Brant and E. A. Svistova: J. Low Temp. Phys. 2 (1970) 1.
- 16) L. Voisin, Y. Guldner, J. P. Vieren, M. Voos, C. Benoit a la Guillaume, N. J. Kawai, L. L. Chang and L. Esaki (this conference).
- 17) L. L. Chang, G. A. Sai-Halasz, L. Esaki, and R. L. Aggarwal (to be published).
- 18) E. E. Mendez, C-A. Chang, L. L. Chang, L. Esaki, and F. H. Pollak (this conference).